Measurement of Nonlinear Normal Modes using Mono-harmonic Force Appropriation: Experimental Investigation

David A. Ehrhardt
Graduate Research Assistant
Department of Engineering Physics, University of Wisconsin-Madison, Madison, WI 53706
dehrhardt@wisc.edu

Matthew S. Allen
Associate Professor
Department of Engineering Physics, University of Wisconsin-Madison, Madison, WI 53706
msallen@engr.wisc.edu

Timothy J. Beberniss
Aerospace Structures Engineer
Structural Sciences Centers, Aerospace Systems Directorate, Air Force Research Laboratory,
Wright-Patterson AFB, OH 45433

Abstract

A structure undergoing large amplitude deformations can exhibit nonlinear behavior which is not predicted by traditional linear theories. Structures with some initial curvature offer an additional complication due to buckling and snap through phenomena, and can exhibit softening, hardening and, internal resonance. As a structure transitions into a region of nonlinear response, a structure's nonlinear normal modes (NNMs) can provide insight into the forced responses of the nonlinear system. Mono-harmonic excitations can often be used to experimentally isolate a dynamic response in the neighborhood of a single NNM. This is accomplished with an extension of the modal indicator function and force appropriation to ensure the dynamic response of the structure is on the desired NNM. This work explores these methods using two structures: a nominally-flat beam and a curved axi-symmetric plate. Single-point force appropriation is used by manually tuning the excitation frequency and amplitude until the mode indicator function is satisfied for the fundamental harmonic. The results show a reasonable estimate of the NNM backbone, the occurrence of internal resonance, and couplings between the underlying linear modes along the backbone.

Keywords: Nonlinear Normal Mode, Experimental Force Appropriation, Continuous Scan Laser Doppler Vibrometry (CSLDV), Digital Image Correlation (DIC)

1 Introduction

Over the past several decades a suite of testing and modeling approaches, under the title of modal analysis, has been developed for linear structures under dynamic loading. The term linear is important here since characterization of a structure using modal analysis is based on quantifying the structure in terms of invariant properties inherent to the structure. With the quantification of these structural properties, (e.g., resonant frequencies, damping ratios, mode shapes, etc.) a complex structure can be described with a small number of known variables in linear response regimes. However, these properties lose their invariance when a structure is in a nonlinear response regime caused by large amplitude loading conditions (thermal, acoustic, mechanical, etc.). Therefore, techniques created for linear structures can not be directly applied to nonlinear behavior since the structural properties become functions of input energy. An understanding of this energy dependent behavior informs the design of critical components and can be exploited to dissipate energy throughout the structure or aid in failure prediction. So new

experimental methods are sought to address nonlinear behavior while preserving the simplicity and connection to the linear design and test paradigms.

Linear experimental modal analysis techniques can be classified into two groups: phase separation and phase resonance methods. There are certainly other classifications of modal analysis techniques, but this is done for convenience of the following discussion. The most popular and easiest implemented methods available today for linear structures are phase separation methods, which excite several or all linear normal modes of interest at a single time with the use of broadband or swept-sine excitation. The modes of vibration can be separated in these measurements using the phase information between the input force and measured response allowing the assessment of natural frequencies, mode shapes, and damping ratios. A good reference for this type of testing and analysis can be found [1, 2]. In contrast, phase resonance testing methods [3-5] for linear structures focus on a single mode of vibration using a multi-point mono-harmonic forcing vector, and are less popular in linear experimental modal analysis because they can be time-consuming. With phase resonance, a mode of vibration is isolated in a test when the phase relationship between the applied harmonic force and measured displacement response fulfills phase lag quadrature. In other words, all degrees of freedom displace synchronously with a phase lag of 90 degrees from the harmonic input force.

The use of these methods with nonlinear vibrations require an extended definition of a mode of vibration since a nonlinear mode is energy dependent and can involve complex interactions between modes. Rosenberg [6] initially defined a nonlinear normal mode (NNM) as a *synchronous solution* of the nonlinear system, but this definition has been extended to include *not necessarily synchronous solutions* of the conservative nonlinear equations of motion [7, 8]. Oscillations of this nature provide significant insight into the structure's free and forced responses, including complex dynamics such as bifurcations, internal resonances, and a strong dependence on input energy. Additionally, the damped dynamics of the system can often be interpreted based on the topological structure and bifurcations of the NNMs of the underlying un-damped system.

The extension of phase separation techniques to characterize a structure's nonlinear response has seen much attention in the form of system identification as shown in [9, 10] which is by no means a complete list of references. Developed phase separation methods have not been readily applied to industrial practice except for low order systems. Phase resonance methods have been extended to the measurement of NNMs through the implementation of different methods of force appropriation. Atkins et al [11] presented a force appropriation of nonlinear systems (FANS) method using a multi-point multi-harmonic force vector to isolate a linear normal mode (LNM) of interest. This permits the direct nonlinear characteristics of the isolated mode to be calculated without modal coupling terms. Peeters et al [12, 13] showed that a multi-point multi-harmonic sine wave could isolate a single NNM. For application to real world structures, it was then demonstrated that a single-point single harmonic force could be used to isolate a response in the neighborhood of a single NNM with good accuracy [12, 14]. In these investigations, once phase lag quadrature was met, the input force was turned off and the response allowed to decay tracing the backbone of the NNM. Building off of this work, Ehrhardt et al [15] used step sine testing to measure the response around a specific NNM and at several input forcing levels leading to nonlinear frequency response functions (FRFs). From these FRFs, responses in the neighborhood of the NNM can be isolated from measured responses.

This investigation focuses on measuring the first linear normal mode of a flat beam and curved axi-symmetric plate and its nonlinear continuation on the NNM at higher energies. Modal interactions from internal resonances are also detected but not rigorously isolated since the main NNM backbone is the primary focus of this investigation. The next section provides some background information regarding NNMs including important characteristics and expected NNMs from finite element models (FEMs). An examination of force appropriation and its application to experimentally isolate an NNM is also presented. Section 3 offers a description of

the geometric properties of both structures and Section 4 then discusses results from the application of force appropriation to the measurement of NNMs for both structures.

2 Nonlinear Normal Modes

2.1 Numerically Calculated NNMs

For an in-depth description of NNMs, their fundamental properties, and methods of calculation, the reader is referred to [7, 8]. Of interest, NNMs have been shown to capture complicated dynamics such as bifurcations, modal interactions, and large energy dependence of the fundamental frequency of vibration. These characteristics can be presented compactly in a frequency-energy plot (FEP) where the change in fundamental frequency of vibration is presented as a function of input energy. Due to these appealing characteristics, much has been done to expand and apply the NNM concept to finite element models (FEMs) [16, 17].

In previous works, finite element models were created for the structures studied here: the flat clamped-clamped beam in [16] and the curved axi-symmetric plate from the exhaust system of a large diesel engine in [15]. Results from the calculation of the first NNM for both of these models is shown in Figure 1 and Figure 2. For reference, a demarcation is added to these plots showing where a maximum displacement of the structure would be equal to one thickness of the structure (eg. 0.76mm for the beam and 1.52mm for the plate).

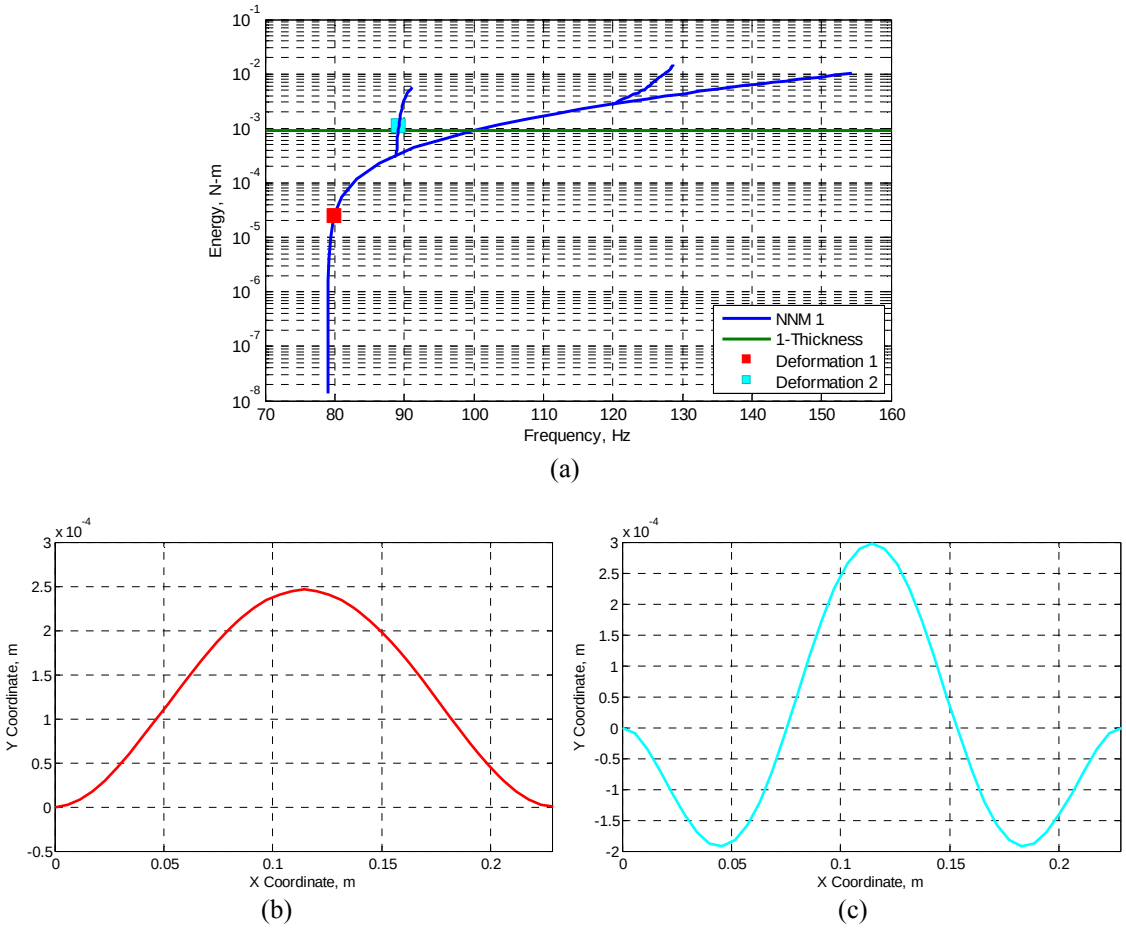

Figure 1: Numerical NNM 1 for flat clamped-clamped beam- a) Frequency-energy plot, b) Deformation 1 shape, c) Deformation 2 shape

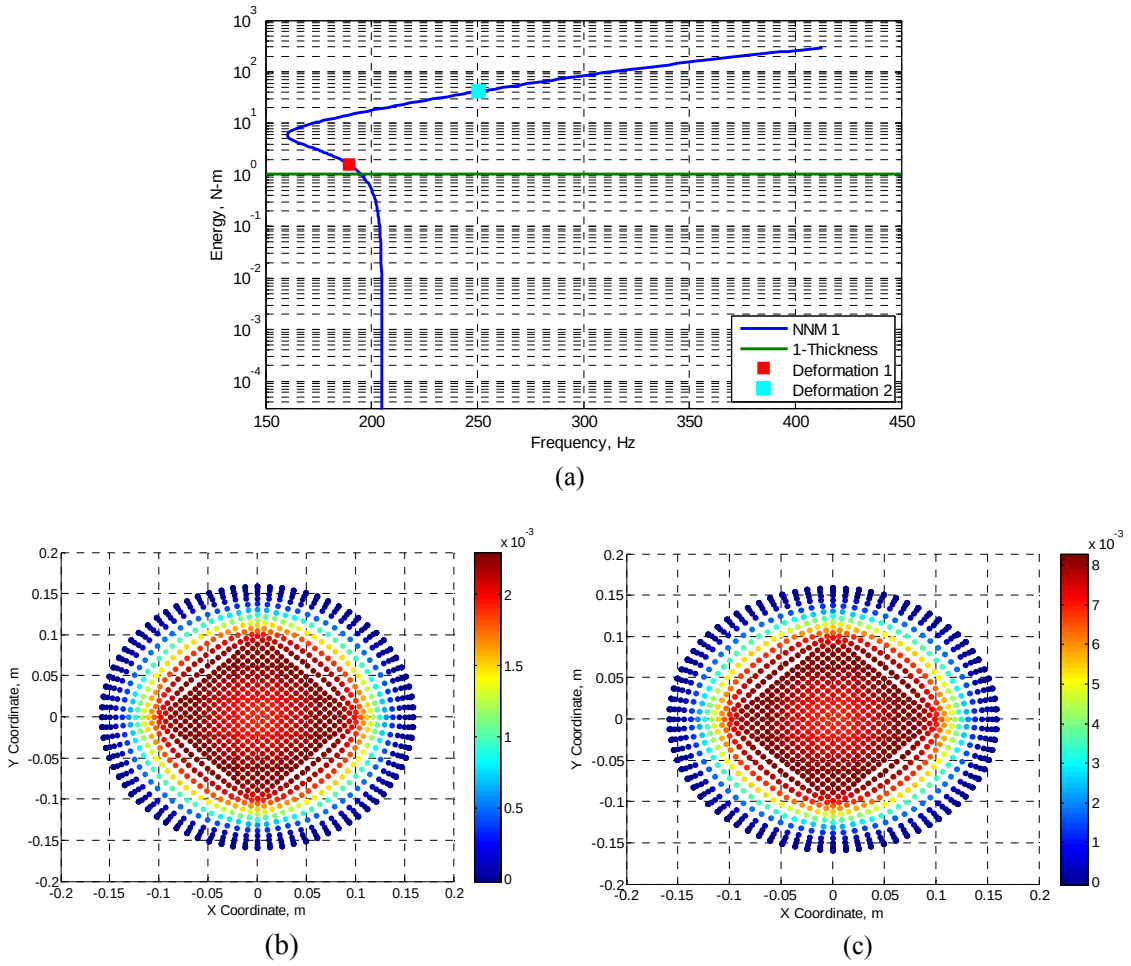

Figure 2: NNM 1 for axi-symmetric plate - a) Frequency-energy plot, b) Deformation 1 shape, c) Deformation 2 shape

As seen in the FEP presented in Figure 1a, the flat beam shows a characteristic spring hardening, or an increase in fundamental frequency of vibration with increased input energy as discussed in [18, 19]. The large change in fundamental frequency of vibration is captured on the backbone of the NNM and is observed for relatively small input energies. Two regions of internal resonance appear as branches off of the backbone curve, also observed in Figure 1a. These branches indicate 5:1 (near 88Hz) and 12:1 (near 120Hz) internal resonances in the response of the beam. For comparison with experimental measurements, it is helpful to examine the deformation of the beam at points along the FEP which are indicated in Figure 1a. Deformation 1, shown in Figure 1b, resembles a mode shape for the first natural frequency of a clamped-clamped beam showing little change in linear shape at this low energy. Deformation 2, shown in Figure 1c, resembles a mode shape for the third natural frequency of a clamped-clamped beam showing the effect an internal resonance has on the overall deformation of the beam. The mode 3 shape becomes more pronounced at higher energies on the internal resonance branch, and less pronounced at lower energies on the internal resonance branch. So, while the mode 3 shape is not dominant at lower energies, the interaction between these modes is still visible as will be shown in the experimental results for this NNM.

Figure 2a shows the first NNM FEP for the curved axi-symmetric plate. The numerically calculated backbone was determined with a reduce-order model (ROM) where the continuation of the first linear normal mode to higher energies was isolated. While this removes the ability to

calculate internal resonances in the plate, this one mode ROM still provides insight into the frequency-energy dependence of NNM 1. As observed here, the NNM undergoes a change in the characteristic nonlinearity as the fundamental frequency of vibration undergoes a decrease prior to increasing. This softening to hardening characteristic can commonly be found in curved structures [20, 21]. Similar to the flat beam, deformations of the plate can also be examined at points along the FEP. Since only mode 1 was used to calculate the NNM, Deformation 1 and 2, shown in Figure 2b and c, are purely mode 1 shapes with different scale factors. The effect of higher modes on an initially flat axi-symmetry plate was examined numerically in. Modes 1 and 6 were both found to be important to describe the response along the NNM backbone providing insight to possible modal interactions.

2.2 Measuring NNMs with Force Appropriation

The implementation of force appropriation to isolate a NNM requires an extension of the phase lag quadrature as discussed in [13] and is repeated here for clarification. The nonlinear forced response of a structure with viscous damping can be represented in matrix form by Eq. (1), where [M] is the mass matrix, [C] is the damping matrix, [K] is the stiffness matrix, f_{nl} is the nonlinear restoring force that is a function of $x(t)$, and $p(t)$ is the external excitation. An un-damped NNM is defined as a periodic solution to Eq. (2), and is the response of the system in Eq. (1) when Eq. (3) is satisfied for all response harmonics. Simply stated, the response of a structure is on the NNM when the forcing function exactly cancels the damping forces in the structure. This approach was used on the clamped-clamped beam studied in this work.

For the circular plate, an inertial load (base excitation) was used where the displacement of the structure is proportional to a rigid body mode, $\psi_{RB}a_b(t)$, so the negative of the base acceleration is shown to be equal to $[C]\{\dot{x}(t)\}$, and hence there is a certain phase relationship between the velocity of the structural response and the base acceleration. The phase relationship between input force and velocity response can be determined by writing the displacement and velocity as Fourier cosine and sine series as shown in Eq. (4). From the defined relationships, an appropriated force is obtained when the applied base acceleration is 180 degrees out of phase with the response velocity. Methods of force appropriation to experimentally isolate a NNM have been used with success on a beam with localized nonlinearity [12], an aircraft with nonlinear joints [14], and an axi-symmetric plate [15]. A structure is defined to respond on an isolated NNM when all harmonics of the response fulfill the phase lag criterion. Building on this work, and the methodology of NNM calculation presented in [17], force appropriation is experimentally applied using a mono-harmonic excitation to isolate the response of the structures in the neighborhood of the desired NNM. For one NNM, the response of the structure is first isolated in the linear range at low energy. After measurement, an increase of input energy is made and the input frequency is adjusted until the phase lag criterion is fulfilled again. Subsequent increase of input energy and changes of frequency are then made until the range of response for the desired NNM is measured.

$$\mathbf{M}\ddot{\mathbf{x}}(t) + \mathbf{C}\dot{\mathbf{x}}(t) + \mathbf{K}\mathbf{x}(t) + \mathbf{f}_{nl}\left(\mathbf{x}(t)\right) = \mathbf{p}(t) \tag{1}$$

$$\mathbf{M}\ddot{\mathbf{x}}(t) + \mathbf{K}\mathbf{x}(t) + \mathbf{f}_{nl}\left(\mathbf{x}(t)\right) = 0 \tag{2}$$

$$\mathbf{C}\dot{\mathbf{x}}(t) = \mathbf{p}(t) = -\mathbf{M}\boldsymbol{\psi}_{RB}a_b(t) \tag{3}$$

$$a_b(t) = \sum_{k=1}^{\infty} \{a_k\} \sin(k\omega t)$$
$$\mathbf{x}(t) = \sum_{k=1}^{\infty} \{\mathbf{X}_k\} \cos(k\omega t) \tag{4}$$
$$\dot{\mathbf{x}}(t) = -\sum_{k=1}^{\infty} \{\mathbf{X}_k\} k\omega \sin(k\omega t)$$

3 Structure Description

3.1 Beam Description

The first device under test for this investigation is a precision-machined feeler gauge made from high-carbon, spring-steel in a clamped-clamped configuration previously studied in [22]. The beam had an effective length of 228mm, a nominal width of 12mm, and a thickness of 0.76mm. All presented dimensions are nominal and subject to variation from clamping and stress variations from machining process to obtain the desired thickness. Prior to clamping, the beam was prepared for three dimensional digital image correlation (3D-DIC) and continuous-scan laser Doppler vibrometry (CSLDV) as discussed in [23] and shown in Figure 3. Locations of the initial laser Doppler vibrometry (LDV) measurements are also shown at the center of the beam and 12mm to the left of the first measurement. The clamping force was provided by the two 6.35-28 UNF-2B bolts located on the inside of the clamping fixture, which is the same fixture used in [22]. After clamping the beam to the fixture, a single-input single-output modal hammer test was performed on the beam so natural frequencies and damping ratios could be identified. Results for the first seven modes are shown in Table 1.

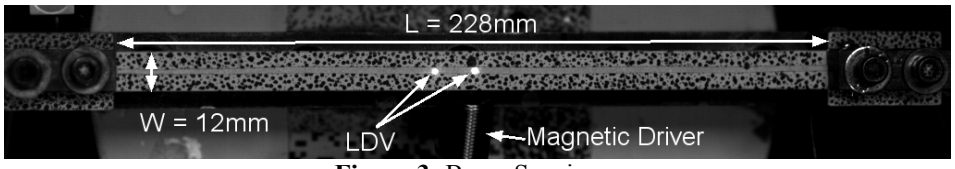

Figure 3: Beam Specimen

Table 1: Linear (low amplitude) natural frequencies of flat clamped-clamped beam

	Mode 1	Mode 2	Mode 3	Mode 4	Mode 5	Mode 6	Mode 7
f, Hz	63.8	193.4	392.7	659.8	855.9	994.1	1396.5
ζ1 , %	0.91	0.25	0.21	0.17	0.12	0.14	0.13

3.2 Plate Description

The second article under investigation is a circular perforated plate with rolled ends which is shown in Figure 4 and previously studied in [15]. A mechanical punch was used to create the circular perforations in a flat 16 gauge (1.52 mm thick) 409 stainless steel plate in an array of equilateral triangles with 10.16 mm long edges. Once this process was completed, the plate was formed around a 317.5 mm diameter mold with the excess trimmed so a lip of 12 mm remained. The plate was then welded to a 89 mm high cylinder made from a 14 gauge (1.9 mm thick) 409 stainless steel plate that was cold rolled to the 317.5 mm diameter as shown in Figure 1b. The welded plate assembly was then bolted to a 317.5 mm diameter by 19 mm thick aluminum fixture with twelve 6.4 mm evenly spaced holes. Figure 4 also shows the location of the single point laser Doppler vibrometers (LDV). After mounting, a single-input single-output modal hammer test was performed on the plate so natural frequencies and damping ratios could be identified. Results for the first nine modes are shown in

Table **2**. CSLDV was not used in this measurement due to the discontinuities from the perforations. It is important to note that all stated dimensions are nominal and subject to variation. Additionally, the processes the plate is subjected to can induce residual stresses in the structure which also might modify the dynamics of the plate in its final configuration. While this system is relatively simple compared to the engine to which it is designed to be attached, work will show how important it is to have a test to validate any computational models that are created; there are a variety of subtle details that might easily be neglected initially, and yet they could change the response considerably.

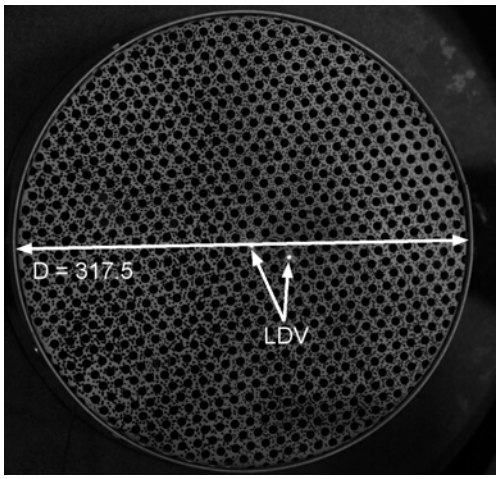

Figure 4: Final Mounted Perforated Plate

Table 2: Linear (low amplitude) natural frequencies of curved axi-symmetric plate

	Mode 1	Mode 2	Mode 3	Mode 4	Mode 5	Mode 6	Mode 7	Mode 8	Mode 9
f, Hz	202.2	324	342.8	489.7	509.9	554.1	697.2	777.9	794.2
$\zeta 1$, %	0.2	0.13	0.31	0.092	0.15	0.087	0.11	0.49	0.43

3.3 Experimental Setup

The final mounted beam and plate are shown in Figure 5. For this experimental setup, there are 3 systems: 1) exciter/controller, 2) full-field measurement systems, and 3) system for force appropriation:

1) Excitation was provided by two separate mechanisms, both controlled in an open-loop using a Wavetek Variable Phase Synthesizer. The beam was excited by a magnetic driver with a Piezo Amplifier. The input force exerted by the magnetic driver was measured using a force transducer mounted to a solid base between the magnetic driver and input location. Due to the weight and size of the curved axi-symmetric plate, the magnetic driver did not produce sufficient force, so excitation was provided by shaking a base on which the plate was mounted with a 5000N MB dynamics shaker and power amplifier. Excitation for this setup is provided through the mounting base at a set excitation acceleration. This type of excitation limits the ability to examine asymmetric modes and keep the plate response in a linear regime.

2) Full-field measurements were taken of the structures using a combination of Continuous-scan laser Doppler vibrometry (CSLDV) and high speed three dimensional digital image correlation (3D-DIC). Details for both of these measurement techniques can be found [23]. Due to the discontinuities of the perforations, CSLDV was only used on the flat clamped-clamped beam.

3) A second laser Doppler vibrometer (LDV) is used to measure the response of the plate as it is subjected to a single frequency sinusoid at a specified excitation amplitude. The voltage

input to the exciter was measured as well as the input force for the magnetic driver and the base acceleration for the shaker. The velocity response and input voltage signals were analyzed in real time using a Onosoki FFT Analyzer to track the phase between the signals. Here, the input voltage was used instead of the measured force/acceleration to limit noise contamination from the measurement sensors. The measured force/acceleration signals were compared after measurement to ensure the correct phase relationship between input and response was maintained. Natural frequencies could then be determined by adjusting the frequency until the input voltage and response velocity are 180 degrees out of phase since the appropriation is between a force and velocity. In a post processing step, the phase relationship for the fundamental harmonic was examined more precisely and the phase relationships for the higher harmonics were computed as well. In the future it would be ideal to be able to monitor all of the phase relationships in real time.

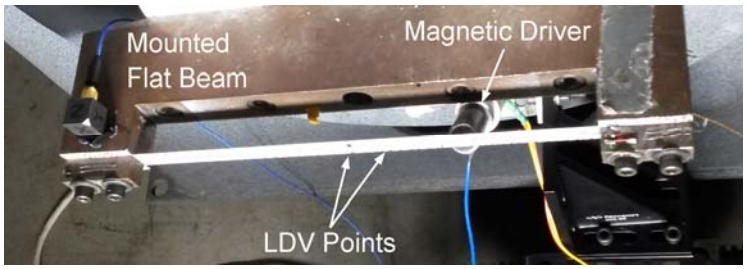

(a)

(b)

Figure 5: Experimental Setup. a) Close up of clamped beam, b) Close up of axi-symmetric plate.

4 Results

4.1 Clamped-Clamped Beam

Using the described methodology and equipment, mono-harmonic force appropriation was used to measure the first NNM of the flat clamped-clamped beam and a curved axi-symmetric plate. The structural response was measured at each appropriated force amplitude once steady-state was achieved. Figure 6 shows the resulting FEP for the flat clamped-clamped beam with the energy of the system represented by the maximum velocity of the beam measured 12mm left of center and plotted against the fundamental frequency of vibration. Similar to the numerically calculated FEP, a large spring hardening characteristic is observed as the beam response approaches a beam thickness. The experimental results show a 36Hz change (or a 50% shift in frequency) when the response amplitude approaches the beam thickness. For comparison,

the numerical results show a 22Hz change. However, no effort was made to tune the boundary conditions in the numerical model to match those in the experiment, so some disagreement is to be expected. Though measured and predicted backbones vary significantly, it is interesting that both show a 5:1 modal interaction, which is visible in the measured FEP as a collection of points near 82Hz. Figure 6b and c show the deformation shapes at the selected points on the experimental FEP in Figure 6a, found using CSLDV. The deformation at the point marked Deformation 1 in Figure 6b shows that, at low energy, the response resembles the first linear mode. At the point marked Deformation 2, which is near the bottom of the internal resonance branch, there is a visible change in shape near the root. If measurements were taken further up this modal interaction one would presumably see mode 3 begin to dominate the overall deformation shape of the beam as was predicted by the analytical model, but this was not pursued further here.

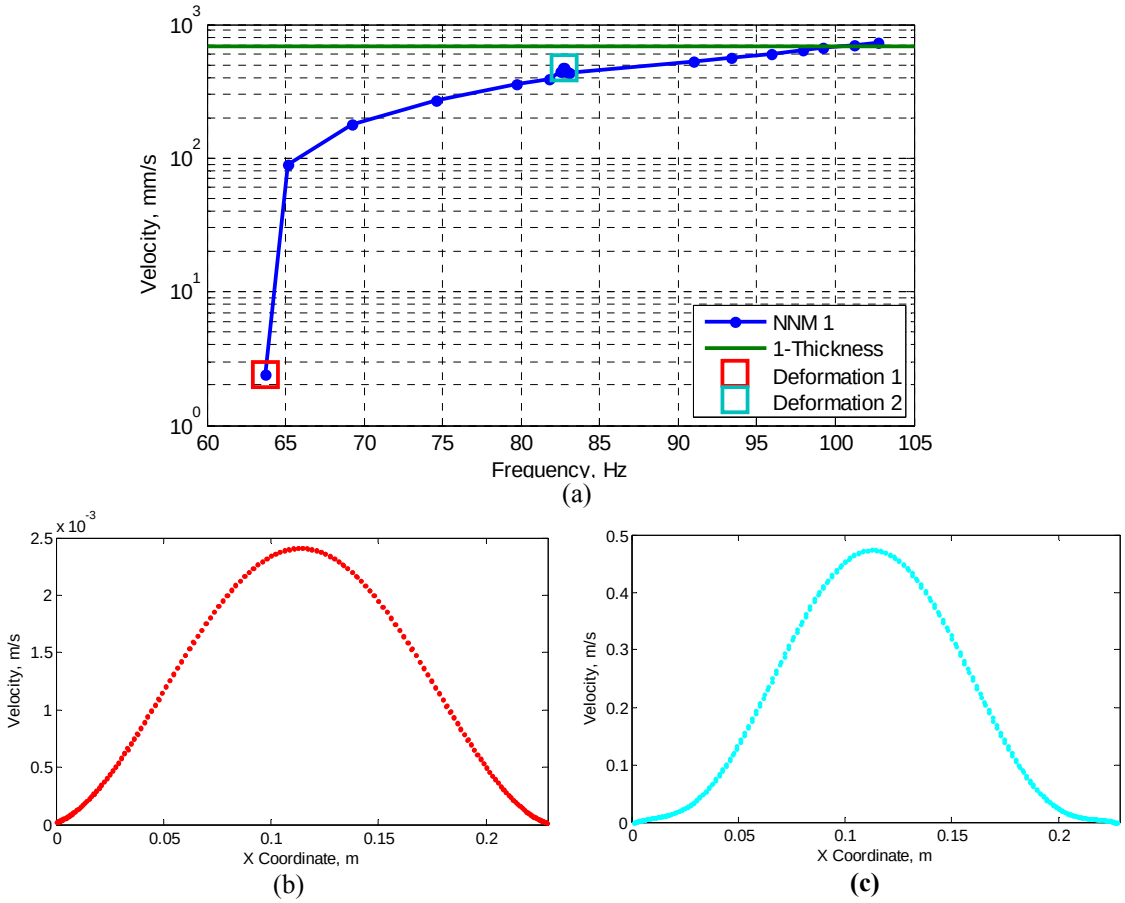

Figure 6: Experimental NNM 1 for flat clamped-clamped beam- a) Frequency-velocity plot, b) Deformation 1 shape, c) Deformation 2 shape

The conclusion that the jump in the data near 82Hz is a modal interaction can be verified by an examination of the spectral content. The amplitude of the fast-Fourier transform (FFT) coefficients of the first seven harmonics is shown in Figure 7a. The evolution of the amplitudes of the higher harmonics show where the 5:1 modal interaction occurs at a 30% change of frequency in the measured NNM. The presence of the modal interaction is predominant in the third, fifth, and seventh harmonics of the response. In these harmonics, larger amplitudes are observed when the response is in the region of the modal interaction, and the amplitude decreases once the response has passed the modal interaction where the 5th and 3rd harmonic show more

dominance. Since single-point mono-harmonic force appropriation is used, an examination of the phase of the harmonics of the response with the input force is important to determine the quality of appropriation. Figure 7b shows how the phase of the first seven harmonics evolve throughout the test, where a phase of -180 degrees would be perfect appropriation since force and velocity are examined. As expected, the first harmonic shows good appropriation throughout measurements except when the response is near the modal interaction and near the initial linear region of the test. Since the modal interaction includes a greater contribution of higher harmonics in the global response of the beam, difficulty of appropriation might be expected in this region. Difficulty of appropriation at lower amplitudes could be due to noise contamination of the velocity measurements at low response amplitudes. The remaining harmonics show a large variability of appropriation due to the use of mono-harmonic force appropriation, but could presumably be improved if higher-harmonic inputs were added to the forcing signal. Indeed, in the simulation study in [17] Kuether found that it was necessary to include higher harmonics to isolate an NNM if the energy was sufficiently high. At even higher energies it also became important to apply a multi-point force.

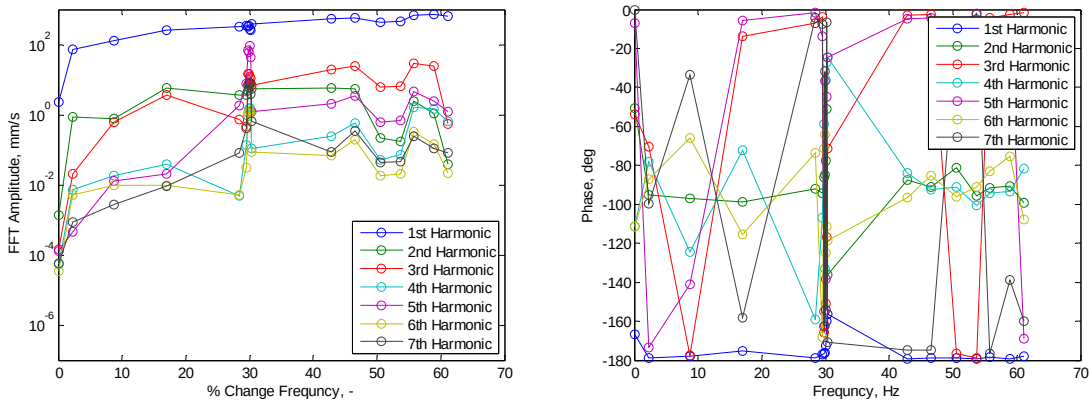

Figure 7: NNM results for the flat clamped-clamped beam - a) FFT amplitude of harmonics in the response and b) Phase results of harmonics in the response

A useful examination of how the deformation of the beam evolves at each harmonic along the backbone curve can be made with the use of full field measurements. Figure 8a-h shows a selection of normalized deformation patterns along the beam for selected harmonics. These shapes could be decomposed into the modes of the structure in order to determine how modal interactions change along the backbone. Figure 8a-g describe how the first seven harmonics of the response change with increasing frequency. The second plotted line (green) shows the harmonic response at the modal interactions previously discussed. Figure 8a shows how the first harmonic evolves from the lowest energy on the backbone curve to the highest with minimal variation from mode 1 of the beam. The line corresponding to the modal interaction is not shown here since the harmonic deformation changes little. Figure 8b shows how the second harmonic transitions from a predominantly mode 1 deformation to a mode 2 deformation where a large skew of mode 1 is observed at the modal interaction. Figure 8c shows a similar result for the third harmonic, where the deformation transitions from a mode 1 deformation to a higher mode of deformation. For the higher harmonics, shown in Figure 8e-g, the dominant response has the shape of mode 3, which continues to higher odd harmonics (9th and 11th), shown in Figure 8h. Figure 8h also shows shapes for the 8th and 10th harmonics at their maximum values which correlate to higher order mode shapes of a beam.

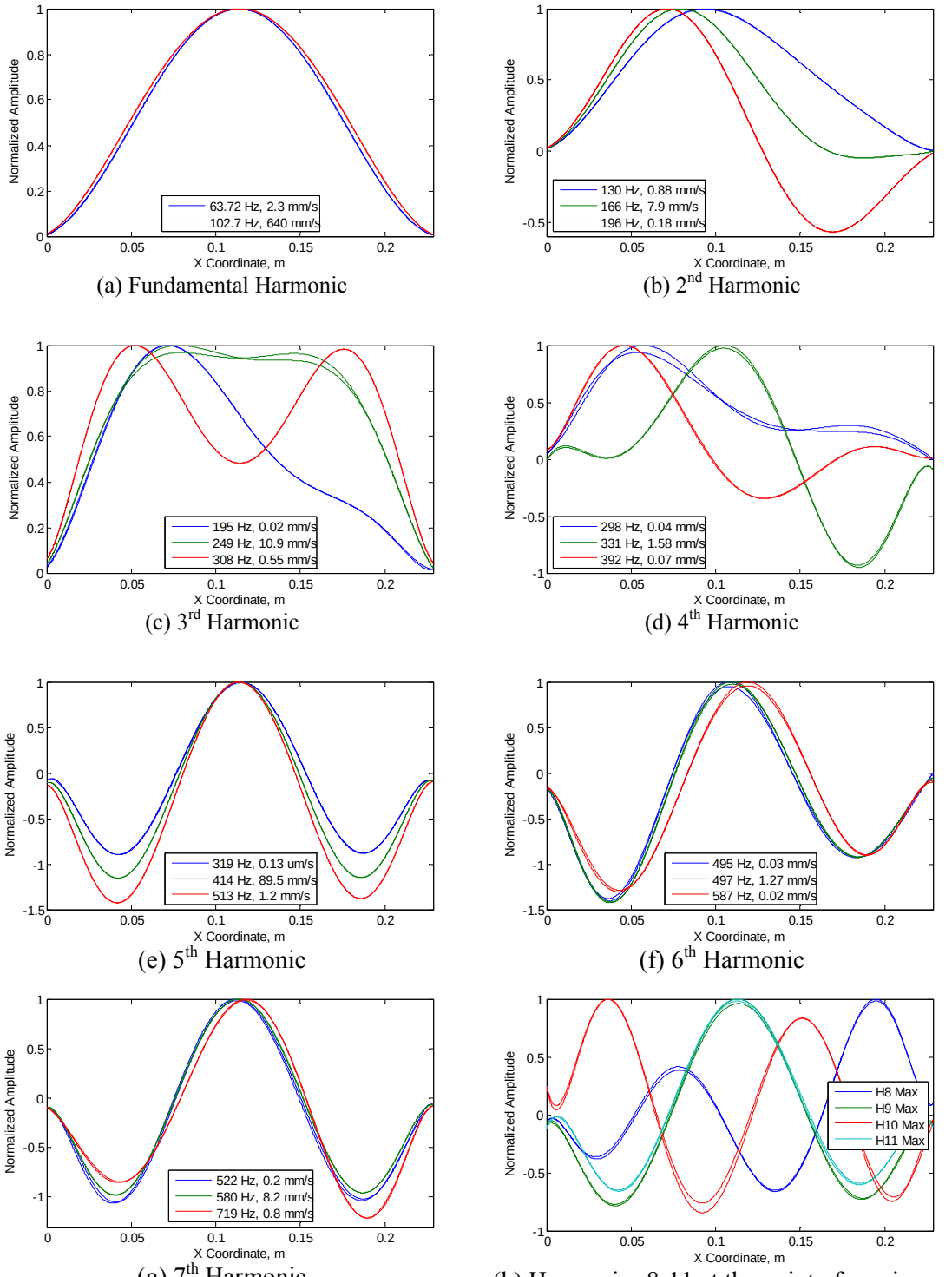

(a) Fundamental Harmonic

(b) 2nd Harmonic

(c) 3rd Harmonic

(d) 4th Harmonic

(e) 5th Harmonic

(f) 6th Harmonic

(g) 7th Harmonic

(h) Harmonics 8-11 at the point of maximum deformation.

Figure 8: Deformation pattern for each harmonic in the response of the beam at three points along backbone curve. The legend shows the frequency from which these harmonics were extracted and the peak velocity amplitude in each shape. The peak velocities can be compared with those of the 1st harmonic to assess the relative importance of each shape to the overall deformation.

The results presented above provide a wealth of information regarding the frequency-energy behavior of the structure and the way in which the deformation evolves with increasing energy. This information can be critical when seeking to develop a model to correctly simulate the response of the structure.

4.2 Circular Plate

Figure 9 shows the experimentally measured NNM of the curved axi-symmetric plate with the velocity response measured at the LDV point located at the [x,y] coordinates of [0.01,-0.03]. Similar to the numerically calculated NNM in Figure 9b, the experimentally measured NNM shows the characteristic spring softening to hardening effect or a decrease of the fundamental frequency of vibration which begins to increase at a specific input force level. Unfortunately, limited data was gathered on the structure in the linear region of response due to inadequate capabilities of the shaker to obtain lower forcing amplitudes. Also, the plate cracked when a higher input force amplitude was attempted, so further testing at low amplitudes was impossible. Failure initially occurred at the [x,y] coordinates of [-0.01,-0.01] which can be identified in Figure 9c & d. With the use of high speed 3D-digital image correlation, maximum deformation shapes of the plate at low and higher energy are shown in Figure 9b-e. Figure 9b & c show the deformation shape at the low energy point marked “deformation 1” in Figure 9a. The deformation at this frequency-energy point resemble mode 1 of a flat plate as expected in linear results. Figure 9d & e show the deformation shape at the high energy point, or deformation 2 also shown in Figure 9a.

To obtain further insights, the measured response is decomposed into its harmonics in Figure 10a. Interestingly, this shows that while the fundamental harmonic is dominant at low amplitude, as the response begins to turn from softening to hardening the harmonics become large, the third harmonic in particular being equal to the first. Hence, while no internal resonances are present the response of this NNM is multi-modal along the backbone. Unfortunately, the phase of the harmonics, shown in Figure 10b reveal that the higher harmonics for the plate are not in quadrature and so one cannot be sure that the NNM has been isolated. The first harmonic stays near 180 degrees phase, but it is less accurate in the spring hardening regime. This is most likely due to the increase of modal interaction at this point. The phase is worse than expected for all harmonics, but the reason is not fully understood at this time.

The full field deformation shapes were again computed for each harmonic to better understand the evolution of the response along the backbone, and are shown in Figure 11. It is particularly interesting to note that the response near the 3^{rd} harmonic takes on a shape similar to the 6^{th} linear mode of the plate. In [24] a finite element model of a similar plate (but with no initial curvature) was studied and linear Modes 1 and 6 were both found to be important to describe the response along the NNM backbone. At the highest level on the FEP, the measurements show that the magnitude of this shape is on the same order of the fundamental harmonic. It is also interesting to note the broadening of the deformation shape around the first harmonic of deformation 1 and deformation 2 , shown in Figure 11a & b. The 5^{th} harmonic, which becomes important only at the last point computed on the NNM. The shapes of the 4^{th} and 5^{th} harmonics suggests that a complicated response occurs in this regime with the inclusion of multiple higher order mode shapes, and this may have been a factor contributing to the failure of the plate.

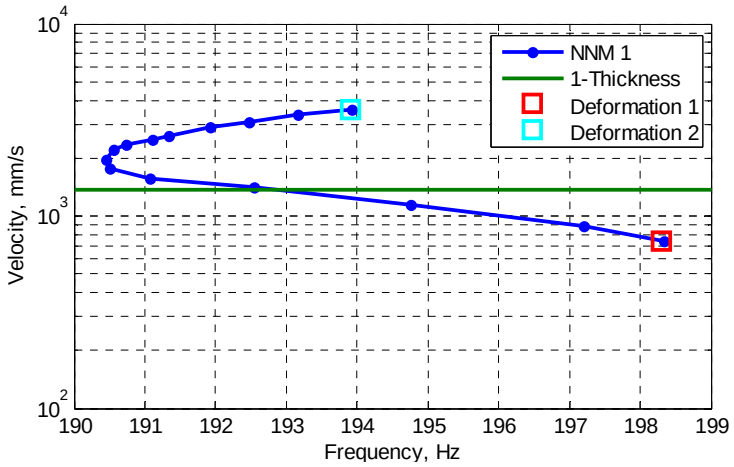

(a)

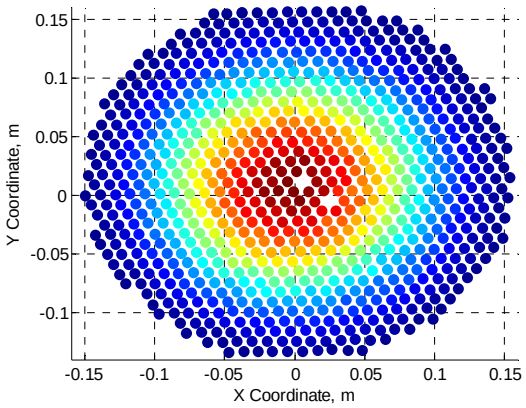

(b)

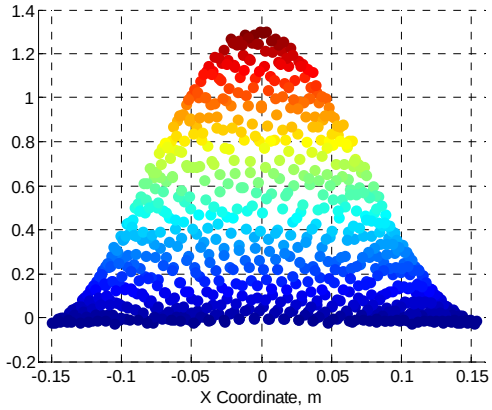

(c)

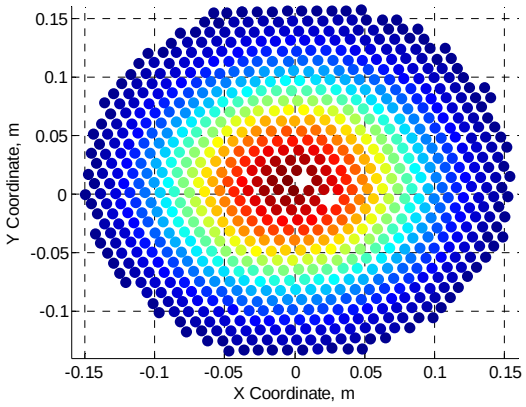

(d)

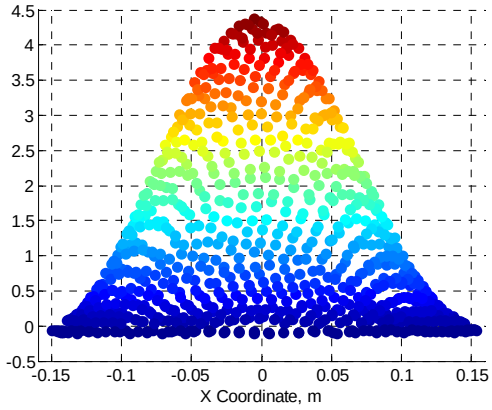

(e)

Figure 9: Experimental NNM 1 for axi-symmetric plate- a) Frequency-velocity plot, b) Deformation 1 shape, c) Deformation 2 shape

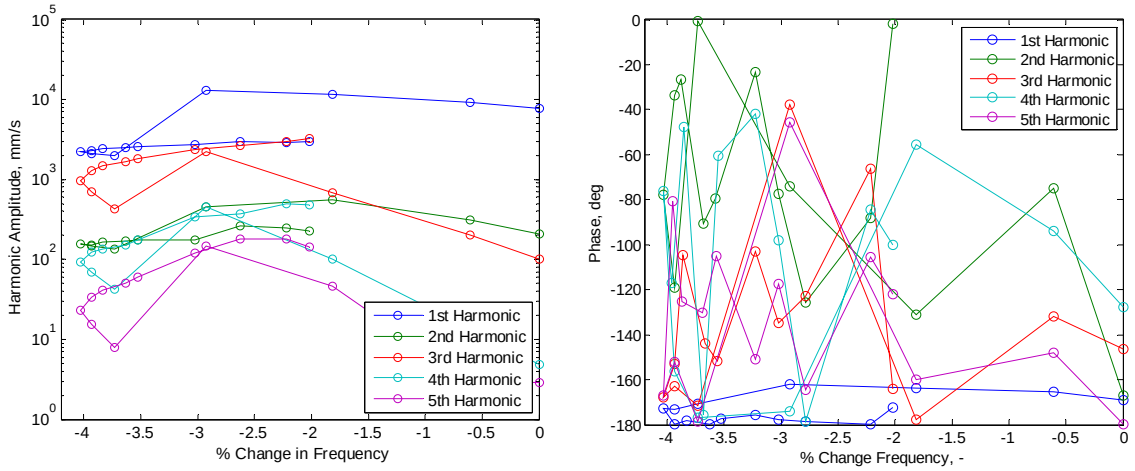

(a) (b)

Figure 10: NNM results for the axi-symmetric plate - a) FFT amplitude of harmonics in the response and b) Phase results of harmonics in the response

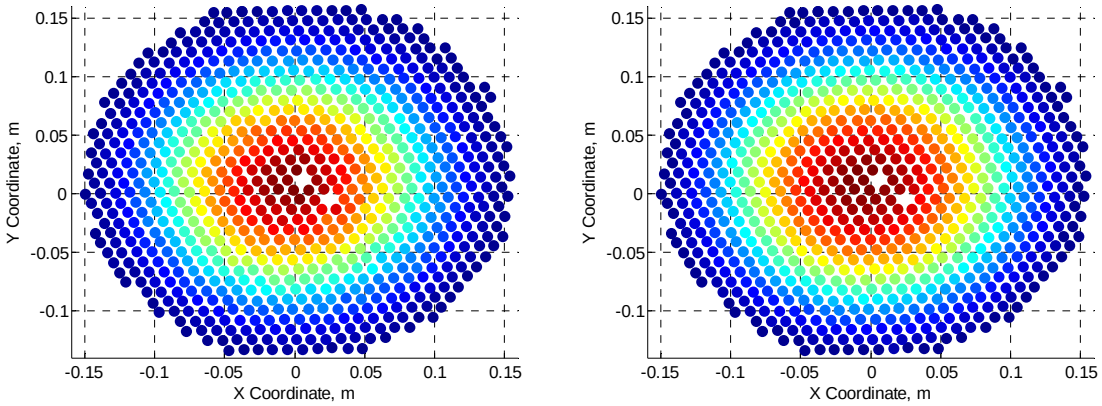

(a) Def 1, 1st harmonic

(b) Def. 2, 1st harmonic

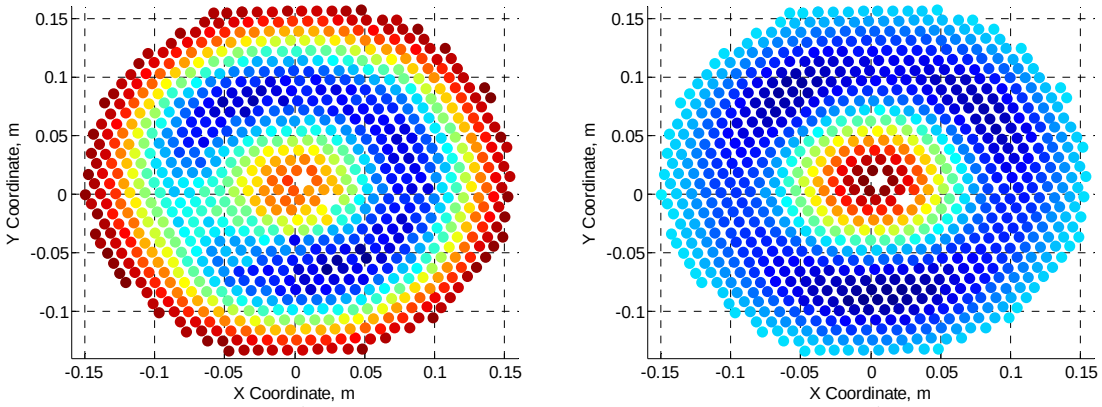

(c) Def. 2, 2nd harmonic

(d) Def. 2, 3rd harmonic

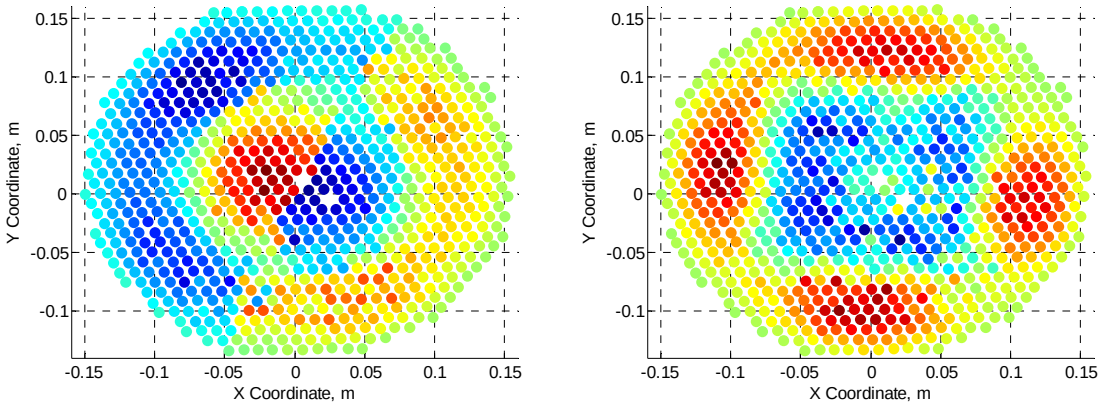

(e) Def. 2, 4th harmonic (f) Def. 2, 5th harmonic

Figure 11: Deformation patterns of plate at various harmonics for two points along the backbone curve: a) 1st harmonic of deformation 1, b-f) 1st harmonic, 2nd harmonic, 3rd harmonic, 4th harmonic, and 5th harmonics respectively of deformation 2

5 Conclusion

The results shown here demonstrate the capability of mono-harmonic force appropriation in two structures exhibiting rich dynamics. The measured response of the flat beam shows the ability to achieve a quality dynamic response in the neighborhood of the beam's first NNM with only mono-harmonic force. In addition to capturing the expected frequency-energy relationship, a modal interaction between the first and third mode of the beam was identified, though not isolated. The measured response of the curved axi-symmetric plate also showed the ability to achieve a dynamic response in the neighborhood of the first NNM of a more complex structure. The quality of the appropriated response for the plate was not on the same level of the beam when looking at the phase of the input and response possibly demonstrating a limitation of a mono-harmonic force to appropriate the response in the neighborhood of the expected NNM.

More work is needed to extend this method of force appropriation for complex structures possibly incorporating multi-harmonic and/or multi-point inputs. As the method of appropriation becomes more complex, higher harmonic amplitude and phase relationships would need to be distinguished in-situ to tune the appropriation. However, even with the relatively simplistic appropriation methodology demonstrated here, results show an adequate identification of the frequency-energy relationship of a structure and insight to modal interactions. So, small improvements in the force appropriation could greatly increase the ability to measure higher energy responses and isolation of modal interactions.

6 References

[1] D. J. Ewins, *Modal Analysis Theory, Practice, and Application*, Second Edition ed.: Research Studies Press Ltd., 2000.

[2] R. J. a. B. Allemang, D.L., "A Unifid Matrix Polynomial Approach to Modal Identification," *Journal of Sound and Vibration,* vol. 211, pp. 301-322, 1998.

[3] R. C. a. W. Lewis, D.L., "A System for the Excitation of Pure Natural Modes of Complex Structure," *Journal of the Aeronautical Sciences (Institute of the Aeronautical Sciences),* vol. 17, pp. 705-722, 1950/11/01 1950.

[4] B. Fraeijs de Veubeke, *A variational approach to pure mode excitation based on characteristic phase lag theory*. Paris, France: North Atlantic Treaty Organization, Advisory Group for Aerospace Research and Development, 1956.

[5] J. R. Wright, J. E. Cooper, and M. J. Desforges, "Normal Mode Force Appropriation - Theory and Application," *Mechanical Systems and Signal Processing,* vol. 13, pp. 217-240, 1999.
[6] R. M. Rosenberg, "Normal Modes of Nonlinear Dual-Mode Systems," *Journal of Applied Mechanics,* vol. 27, pp. 263-268, 1960.
[7] A. F. Vakakis, Manevitch, L.I., Mikhlin, Y.V., Pilipchuk, V.M., and Zeven, A.A., *Normal Modes and Localization in Nonlinear Systems*. New York: John Wiley & Sons, 1996.
[8] G. Kerschen, M. Peeters, J. C. Golinval, and A. F. Vakakis, "Nonlinear normal modes, Part I: A useful framework for the structural dynamicist," *Mechanical Systems and Signal Processing,* vol. 23, pp. 170-194, 2009.
[9] G. Kerschen, K. Worden, A. F. Vakakis, and J.-C. Golinval, "Past, present and future of nonlinear system identification in structural dynamics," *Mechanical Systems and Signal Processing,* vol. 20, pp. 505-592, 2006.
[10] K. Worden, G.R. Tomlinson, *Nonlinearity in Structural Dynamics: Detection, Identification, and Modeling*. Bristol and Philadelphia: Institute of Physics Publishing, 2001.
[11] P. A. Atkins, J. R. Wright, and K. Worden, "AN EXTENSION OF FORCE APPROPRIATION TO THE IDENTIFICATION OF NON-LINEAR MULTI-DEGREE OF FREEDOM SYSTEMS," *Journal of Sound and Vibration,* vol. 237, pp. 23-43, 2000.
[12] M. Peeters, G. Kerschen, and J. C. Golinval, "Modal testing of nonlinear vibrating structures based on nonlinear normal modes: Experimental demonstration," *Mechanical Systems and Signal Processing,* vol. 25, pp. 1227-1247, 2011.
[13] M. Peeters, G. Kerschen, and J. C. Golinval, "Dynamic testing of nonlinear vibrating structures using nonlinear normal modes," *Journal of Sound and Vibration,* vol. 330, pp. 486-509, 2011.
[14] M. Peeters, G. Kerschen, J. C. Golinval, C. Stéphan, and P. Lubrina, "Nonlinear Normal Modes of a Full-Scale Aircraft," in *Modal Analysis Topics, Volume 3*, T. Proulx, Ed., ed: Springer New York, 2011, pp. 223-242.
[15] D. Ehrhardt, R. Harris, and M. Allen, "Numerical and Experimental Determination of Nonlinear Normal Modes of a Circular Perforated Plate," in *International Modal Analysis Conference XXXII*, Orlando, Fl, 2014, pp. 239-251.
[16] R. J. Kuether and M. S. Allen, "A numerical approach to directly compute nonlinear normal modes of geometrically nonlinear finite element models," *Mechanical Systems and Signal Processing,* vol. 46, pp. 1-15, 2014.
[17] R. J. Kuether, Allen, M.S., "Computing Nonlinear Normal Modes Using Numerical Continuation and Force Appropriation," presented at the 24th Conference on Mechanical Vibration and Noise, 2012.
[18] R. W. Gordon and J. J. Hollkamp, "Reduced-order Models for Acoustic Response Prediction," Air Force Research Laboratory, AFRL-RB-WP-TR-2011-3040, Dayton, OH2011.
[19] J. J. Hollkamp and R. W. Gordon, "Reduced-order models for nonlinear response prediction: Implicit condensation and expansion," *Journal of Sound and Vibration,* vol. 318, pp. 1139-1153, 2008.
[20] L. N. Virgin, *Vibration of Axially Loaded Structures*. Cambridge, United Kingdom: Cambridge University Press, 2007.
[21] L. N. Virgin, *Introduction to Experimental Nonlinear Dynamics: A Case Study in Mechanial Vibration*. Cambridge, United Kingdom: Cambridge University Press, 2000.
[22] R. W. Gordon, Hollkamp, J.J., and Spottswood, S. M., "Non-linear Response of a Clamped-Clamped Beam to Random Base Excitation," presented at the VIII International

Conference on Recent Advances in Structural Dynamics, Southampton, United Kingdom, 2003.

[23] D. Ehrhardt, S. Yang, T. Beberniss, and M. Allen, "Mode Shape Comparison Using Continuous-Scan Laser Doppler Vibrometry and High Speed 3D Digital Image Correlation," in *International Modal Analysis Conference XXXII*, Orlando, FL, 2014, pp. 321-331.

[24] R. J. Kuether, B. Deaner, M. S. Allen, and J. J. Hollkamp, "Evaluation of Geometrically Nonlinear Reduced Order Models with Nonlinear Normal Modes," *AIAA Journal,* vol. Submitted August, 2014.